文章编号 1674-2915(2011)04-0388-09

Design and analysis of support structure for typical lens of carbon dioxide detector

LIANG Biao[1,2], LIU Wei[1]

(1. *Changchun Institute of Optics, Fine Mechanics and Physics, Chinese Academy of Sciences, Changchun* 130033, *China*;
2. *Graduate University of Chinese Academy of Sciences, Beijing* 100039, *China*)

Abstract: To decrease the influence of external loads and temperature changes on the surface deformation and alignment of a lens, a typical lens support structure was investigated based on the characteristics and technical requirements of carbon dioxide detectors for optical systems and specifications. A radial support structure was proposed and its 3D model was established. In order to verify the reasonability of the structure, the dynamic and static rigidities as well as thermal characteristics were analyzed by using a nonlinear analysis method through CAD engineering analytical software. The analysis results indicate that the first frequency of lens sub-assembly is 1 301 Hz, and lens surface shape error is as follows: PV ≤ λ/10, RMS ≤ λ/50, Tilt error ≤ 1″. The radial support structure can keep lens centration well and reduce the influence of temperature diversification on the lens surface deformation. These results validate the rationality of structure and satisfy the design requirements.

Key words: carbon dioxide detector; radial support; structure design; finite element analysis

二氧化碳探测仪典型透镜支撑结构的设计及分析

梁 彪[1,2],刘 伟[1]

(1. 中国科学院 长春光学精密机械与物理研究所,吉林 长春 130033;
2. 中国科学院 研究生院,北京 100039)

摘要: 为了降低外界载荷和温度变化对二氧化碳探测仪光学系统透镜面形及共轴的影响,根据系统的特点和技术要求,对其典型透镜的支撑结构进行了研究,设计了一种径向挠性支撑结构并建立了3D实体模型。运用工程CAD分析软件,采用非线性有限元分析方法对其进行了动静刚度特性和热特性仿真分析,验证了支撑结构设计的合理性。分析结果表明,透镜结构组件的一阶固有频率为1 301 Hz;利用面型拟合,得到了各工况下镜面面形误差值为PV≤λ/10,RMS≤λ/50,偏转误差≤1″。该径向支撑结构能很好地保持透镜共轴精度,减小了温度变化对镜面变形的影响,各项结果满足设计要求,证明了结构设计的合理性。

关 键 词: 二氧化碳探测仪; 径向支撑; 结构设计; 有限元分析
中图分类号: TH744.1; X851 **文献标识码:** A

收稿日期: 2011-03-12; **修订日期:** 2011-04-23
基金项目: 国家863高技术研究发展计划资助项目(No. 2010AA1221091001)

1 Introduction

Carbon dioxide is a principal human-made greenhouse gas and the primary atmospheric component of the global carbon cycle. Human activities now emit more than 32 billion tons of carbon dioxide into the atmosphere each year, and the annual emission rate has increased steadily since the drawn of the industrial age. Over half of this carbon dioxide has been absorbed by natural sinks on land and in the ocean and the remainder stays in the atmosphere [1]. Measurements made by the international carbon cycle science community have substantially improved our understanding of CO_2 sources and sinks, and their relationship to the climate change. Despite this progress, knowledge of the location of CO_2 sources and sinks, as well as how it concretely affects the climate evolution continues to be limited by a lack of a high precision global measurement of atmospheric CO_2. Advances in carbon cycle science have intensified the need for accurate global observations of carbon dioxide from space. Therefore, many countries have made extensive researches on the measurements of CO_2. In 2002, NASA selected the Orbiting Carbon Observatory(OCO) to return space-based measurements to measure carbon dioxide sources and sinks [2]. Japanese successfully launched the Greenhouse gases Observing Satellite(GOSAT) in 2009 to measure the global greenhouse gas and provided various data for the predication of global change.

Carbon dioxide detector is used to monitor carbon dioxide globally from space, it aims to the contribute to the international efforts to prevent global warming and find out where the carbon source is and how distributions it is. The carbon dioxide detector measures the intensity of sunlight that has reflected off earth surface and passed through the atmosphere to get spectrum information, then the greenhouse gas content is got by various inversion algorithms [3]. For a high performance carbon dioxide detector, due to the hash working environments and high resolution requirement, it is important to design a appropriate opto-mechanical structure. One of the important aspects is the lens support structure design. Many new types of mirror structures have been proposed [4-6], but there are very few papers research on high performance lens's support structure [7-8]. In this paper, based on the specifications of the biggest typical lens of carbon dioxide detector, a radial support structure for it has been proposed. To verify the new model, the performance under different conditions has been analyzed by using FEA methods. The results show that it satisfies requirements well and has many advantages compared with the general lens support structure.

2 General considerations in opto-mechanical design

One of the principles of structure design is to obtain the lightest mass while assuring the necessary strength and stiffness. The support structure must have enough strength and stiffness to bear the complicated dynamic load and impacting load. Structural design should be adequately rigid that the displacements of the interrelated components and the mechanical stresses imposed there on are smaller than the tolerable limits under all anticipated operational conditions. Fig. 1 is the flow diagram for design phases of lens support structure. Deformations of lenses, housings, and other structural members do occur in the presence of thermal, acceleration, and other externally applied loads. Lens surface deformation and position error have a big influence on detector's performance, so it must be strictly controlled. To ensure the work quality, for the typical lens of the carbon dioxide detector, it is required to be assembled with extremely tight axial, tilt, and decentration tolerances. Alignment must be retained under operational levels of shock, vibration, and temperature variations. Furthermore, misalignments

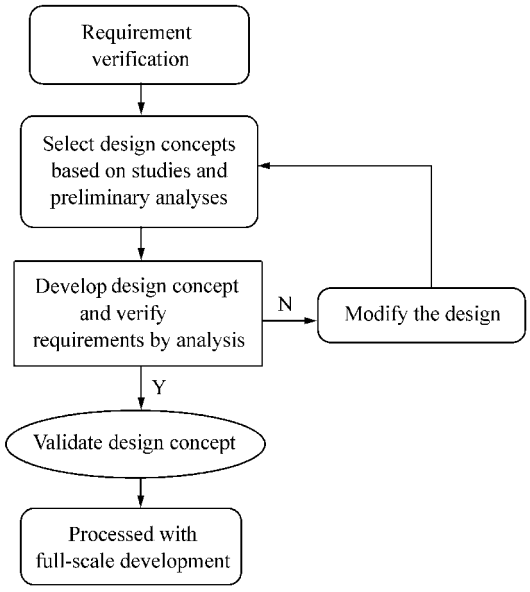

Fig. 1 Flow diagram for design process

occurring during exposure to survival levels of these environments must be reversible. For general support structure, it can not meet these, so a new type of support structure must be developed to meet the requirements above and no to make the differential expansion of materials caused by temperature changes affect lens tilt or centration. Fig. 2 shows the optical structure layout of the detector. The main

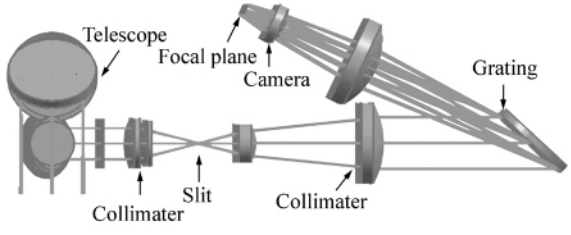

Fig. 2 Optical layout of the detector

Tab. 1 Specifications and tolerances for typical lens

Specifications	Tolerance
Operating temperature	8 ~ 28 ℃
Tilt error	≤ 1″
Decenter error	≤1 μm
P-V	≤λ/10
RMS	≤λ/50

design specifications for typical lens in the support structure under all working conditions are as shown in Tab. 1.

3 Design of lens support structure

3.1 Lens mounting method and opto-mechanical interface

It is based on the application requirements of instrument to lens and lens size to select mounting methods. There are many mounting methods for lens. Burnished mounting is most frequently used with small lens. The cell material must be malleable rather than brittle. It is inexpensive, compact, and requires a minimum number of parts, but the mounting is permanent, removal of the lens without damaging it is extremely difficult. It is very easy to apply permanent stress to lens during the burnishing operation which would cause the decrease of profile accuracy. Another method is the threaded retaining ring mounting, it is widely used in the lens that can not be used with burnished mounting and radius more than 50 mm[9]. Compared with other mounting methods, the stress to lens is minimal and the mechanical reliability is high. In a typical mounting configuration, the main chief variable is the magnitude of applied force and the shapes of the opto-mechanical interfaces between the lens material and metal parts. Sharp corner interfaces and tangential interfaces are most widely used. Compared with sharp corner, easily made by the modern machining technology, the tangential interface tends to produce smaller contact stress in the lens for a given preload than the sharp corner interface. The lens radial flexure support structure uses threaded retaining ring and tangential interfaces based on above.

3.2 Structure design

A modular design is adopted for lenses of the detector, that each of these lenses is contained in it's own individual cell, then it is very convenient to alignment and maintenance. Lens material is silica,

invar was chosen as the support structural material because of it's thermal expansion properties closely matching lens. The structures supporting lens would deform under the thermal effects, gravity load and externally applied loads. It is thus indispensable to isolate the optics to avoid subjecting them to undue stress [9]. This is accomplished by mounting the optics in a statically determinate manner, using what is called a kinematic mount. A rigid body in space has six degrees of freedom: translation and rotation along each of three orthogonal axes. The body is fully constrained when each of these possible movements is singly prevented. If any one movement is constrained in more than one way, then the body will be deformed by the external forces. Kinematic mount is a mounting system which does not constrain more than six rigid-body degrees of freedom. When an optical element is mounted kinematically, the structure supporting can deform in response to a thermal load or changing gravity vector without affecting the optical figure, the optical element can move as a rigid body, but will not deform [10]. One common form of kinematic mount for optical elements is the three point support as shown in Fig. 3. The symbols C_R and C_T in Fig. 3 represent the spring constants(stiffness) of radial and tangential flexures.

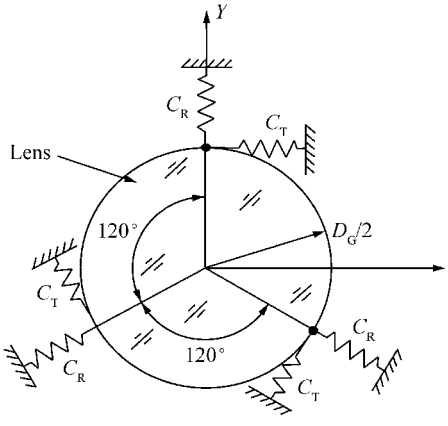

Fig. 3　Schematic of three-point structure

Typically, the flexures are stiff tangentially and axially, soft radially. This configuration has the advantage of minimizing decenter errors even in the presence of large differential contractions between optical elements and their support structures.

Therefore the concept of the radial support structure for lens has been proposed in Fig. 4 and Fig. 5. Three outer convex surfaces are attached to barrel, three inner seats feature at 120 intervals which provide contact surfaces for lens, then six flexure modules have been formed.

Fig. 4　Example of lens radial support

Fig. 5　3-D model of lens radial support structure

The equal compliances of the six radially oriented flexures keep the lens centered in spite of differential expansion with temperature changes, and allow the lens to decent during extreme shock and vibration exposure, yet return to the correct location after these dynamic disturbances have subsided. It also minimizes stress within the optic during such exposures, because it has isolated the optics from support structure. In order to relieve thermal stresses and

preload the system in the direction of the axis, a single O-ring is placed on the surface. Fig. 6 shows example of cell components.

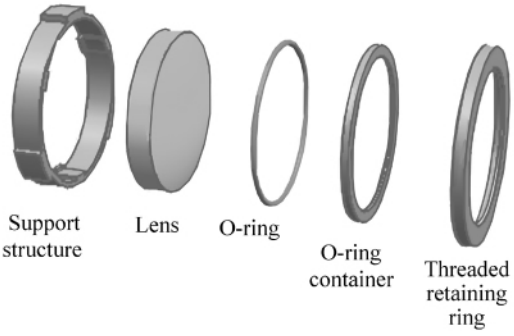

Fig. 6 Cell components with radial support structure

4 Finite element analysis

To verify the model, the dynamic and static rigidities as well as thermal characteristics of the radial flexure support structure were analyzed by using FEA software. Lens cell subassembly is consisted of Cell, lens, O-ring, O-ring container, and threaded retaining ring. The 3-D model of the subassembly is shown in Fig. 7. A nonlinear finite analysis is applied to the support structure subassembly, which uses contact element in the analysis model [11]. Tab. 2 is the material properties of lens radial support structure subassembly.

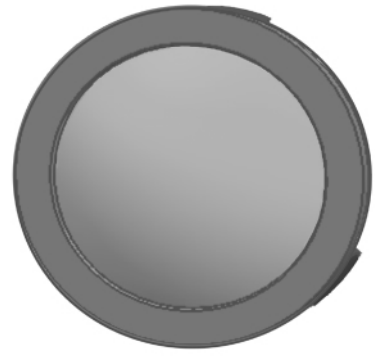

Fig. 7 Three dimensional model of subassembly

Tab. 2 Properties of different materials

Material	Density ρ/(g·cm^{-3})	Young's modulus E/GPa	Poisson's ratio μ	CTE α/($\times 10^{-6}$/℃)
Silica	2.2	67	0.17	0.21
RTV	0.8	0.003 4	0.48	300.6
Invar	4.4	141	0.34	0.31

4.1 Static stiffness analysis

The gravity load is applied in three perpendicular directions of the model to check the static stiffness, the theaim is to find out whether lens surface deformation and position error are in the tolerance limits. Fig. 8 and Fig. 9 are the displacement and stress of the system with one gravity load in the direction of optics axis(axis Z) . The results in the figures show that the maximum displacement is 1.4×10^{-5} mm, the maximum stress is 0.12 MPa. Displacement and stress in other two directions also meet the requirements of tolerance. To evaluate the influence of radial support structure on the lens with the gravity load, it is necessary to calculate lens surface deformation by using the FE results. The surface deformation physically represents the deviation of the deformed optical surface from the undeformed

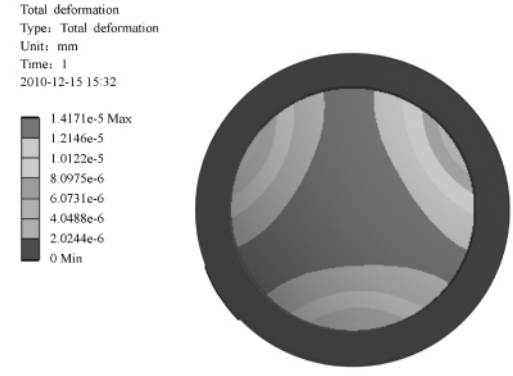

Fig. 8 Displacement of system with gravity load along optics axis

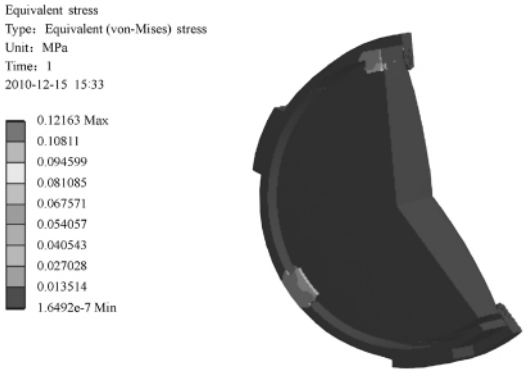

Fig. 9　Stress of the system with gravity load along optics axis

optical surface at each point on the optical surface. Lens surface 1 is the convex surface, surface 2 is the plat surface. The rigid body displacement and tilt of the lens are shown in Tab. 3. The maximum rigid body displacement is 0.013 μm, the maximum tilt is 0.013″, and both are less than the tolerable limit. The P-V and RMS of the lens surface deformation are shown in Tab. 4, and the lens maximum surface shape error RMS is 2.29 nm, less than 12.6 nm.

Table. 3　Rigid body displacements and tilts of lens with gravity load

		Gravity load direction		
		X	*Y*	*Z*
Displacement/μm	Δ*X*	0.012 8	≈0	≈0
	Δ*Y*	≈0	−0.012 9	≈0
	Δ*Z*	≈0	≈0	−0.013
Tilt/(″)	θ_X	≈0	−0.013	≈0
	θ_Y	0.013	≈0	≈0

Tab. 4　Surface shape errors of lens

Gravity direction	Surface type	P-V/nm	RMS/nm
X	Surface 1	0.84	0.12
	Surface 2	1.16	0.16
Y	Surface 1	0.73	0.11
	Surface 2	1.25	0.14
Z	Surface 1	5.73	1.07
	Surface 2	10.52	2.29

The radial support structure can satisfy the static rigidity requirements.

4.2　Dynamic analysis

It is necessary to have a modal analysis to prevent lens subassembly from forced vibration during the launch. The first three order natural frequencies and vibration modes are shown in Tab. 5. The first natural frequency is 1 301 Hz, higher than the specified value 300 Hz, therefore, the lens subassembly would not resonate under the influence of external environments.

Tab. 5　The first three order natural frequencies and vibration modes

Mode	Frequency/Hz	Vibration mode
1	1 301.1	*Z* axis direction
2	1 449.7	*X* axis direction
3	1 468.6	*Y* axis direction

4.3　Thermal analysis

In the case of the space applications, the amplitude of temperature changes can be very large, Temperature change can modify the separation between optical elements and change the figure of the elements . It causes defocus and misalignment, so the support structure must make sure that the decenter as small as possible and minimize the stress and surface deformation of the lens. The detector´s operation temperature is from 8 to 28 ℃ and the fabrication and assembly temperature is 18 ℃, so it is necessary to analyze the subassembly under those extreme temperatures [12]. The FE model is defined with restrictions of temperature of 8 and 28 ℃. Fig. 10 and Fig. 11 are the displacement and stress of the lens subassembly at 8 ℃. Fig. 12 and Fig. 13 are the displacement and stress of the lens subassembly at 28 ℃. When the subassembly is applied at 8 ℃, the maximum thermal stress would appear at the contact area of lens and support structure, because of the different CTEs of the material, as it is shown in Fig. 11, and the maximum stress is 0.31 MPa, which is less than the tolerable limit. The contact

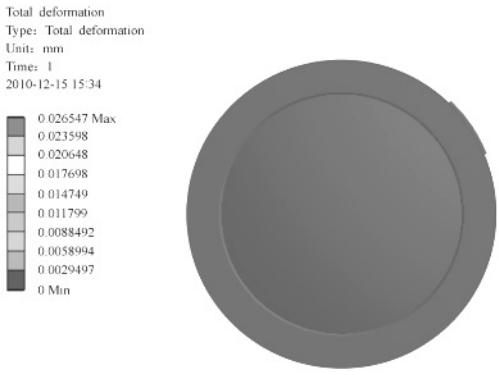

Fig. 10 Displacement of radial support structure subassembly at 8 ℃

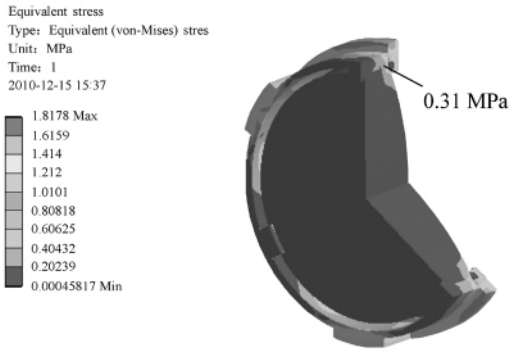

Fig. 11 Stress of radial support structure subassembly at 8 ℃

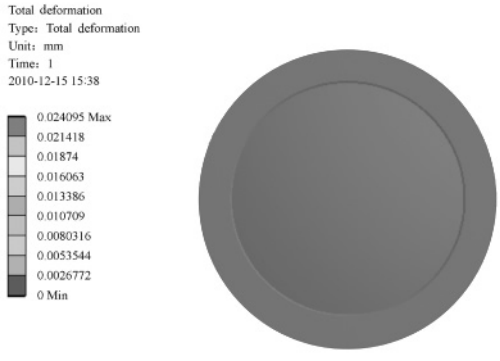

Fig. 12 Displacement of radial support structure subassembly at 28 ℃

between the structure and lens should be free of stress at the temperature of 28 ℃ as shown in

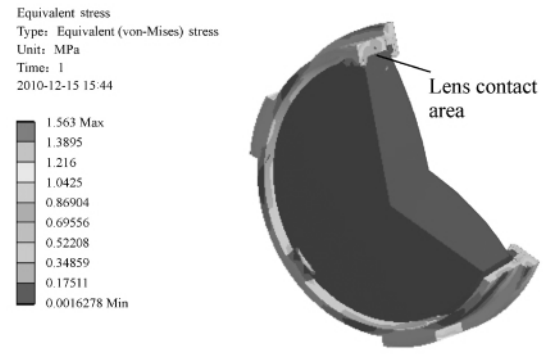

Fig. 13 Stress of radial support structure subassembly at 28 ℃

Fig. 13. To evaluate the influence of lens radial support on the lens with thermal load, lens surface deformation is calculated. Tab. 6 is the rigid body displacement and tilt of lens with thermal load. The maximum rigid body displacement is 0.42 μm, and the maximum tilt is 0.076″, which are less than the tolerable limit. Tab. 7 is lens surface deformation. It shows that the maximum surface shape error RMS is 11.69 nm, which is less than the tolerable value 12.6 nm. Radial support structure is compared with general support structure under the same thermal

Tab. 6 Rigid body displacements and tilts of lens with thermal load

		8 ℃	28 ℃
Displacement/μm	ΔX	−0.004	0.015
	ΔY	≈0	0.019
	ΔZ	0.25	−0.42
Tilt/(″)	θ_Z	≈0	≈0
	θ_Y	−0.002 5	−0.076

Tab. 7 Surface shape error of lens at different temperatures

Temperature	Surface type	P-V/nm	RMS/nm
8 ℃	Surface 1	42.43	7.63
	Surface 2	59.62	11.69
28 ℃	Surface 1	17.81	3.21
	Surface 2	32.6	6.49

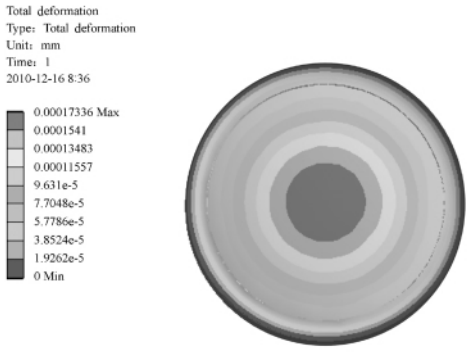

Fig. 14　Displacement of general support structure subassembly at 8 ℃

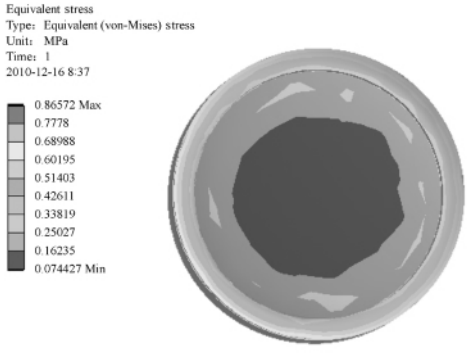

Fig. 15　Stress of general support structure subassembly at 8 ℃

load. Fig. 14 and Fig. 15 are the displacement and stress of general support subas – sembly at 8 ℃, which shows that the stress and deformation are much larger than radial support, and the stress distribution is more uneven. Compared with general support structure, the radial support is more insensitive to temperature change and has a better ability to keep lens alignment.

5　Conclusions

A lens radial support structure was designed on the characteristics and technical requirement of the optical system of a carbon dioxide detector for specifications. To verify the reasonability of the structure, the dynamic and static rigidities as well as thermal characteristics were analyzed. In order to improve the analysis accuracy, a nonlinear finite element was applied. The results show that the lens radial support structure can better keep the lens alignment and more insensitive to the temperature change, and also can effectively reduce the lens surface deformation caused by the gravity load and temperature change. The maximum surface-shape error RMS and the maximum tilt error are 11.69 nm and 0.076″, which are less than the specified value RMS 12.6 nm and 1″, respectively. The radial support structure design is rational, and fully meets the requirements of carbon dioxide detectors.

参考文献:

[1] DAVID C, CHARLES E M, PHILIP L. NASA Orbiting Carbon Observatory: measuring the column averaged carbon dioxide mole fraction from space [J]. *J. Appl. Remote Sensing*, 2008, 023508: 15-50.

[2] DAVID C. The need for atmospheric carbon dioxide measurements from space: contributions from a rapid reflight of the Orbiting Carbon observatory [R]. Pasadena, California: Atmospheric Carbon Dioxide Measurements From Space, 2009, 321: 1-23.

[3] CARL C L, RANDY P, BRETT H, *et al*.. System for establishing best focus for the Orbiting Carbon Observatory instrument [J]. *Optical Eng.*, 2009, 073605: 1-3.

[4] HUANG E W. Gemini primary mirror cell design [J]. *SPIE*, 1996, 2871: 291-300.

[5] KAERCHAER H. The evolution of the SOFIA telescope system design-lessons learned during design and fabrication [J]. *SPIE*, 2003, 4857: 251-260.

[6] BITTER H, ERDMAN M, HABERLER, *et al*.. SOFIA primary mirror assembly: structural properties and optical performance [J]. *SPIE*, 2003, 4857: 266-278.

[7] JOHN J B. Precision lens mounting: US, 4733945 [P]. 1988-04.

[8] AHMAD, HUSE R L. Mounting for high resolution projection lenses: US, 4929054 [P]. 1990-06.

[9] PAULR Y J. *Opto-Mechanical Systems Design* [M]. Boca Raton, Florida: CRC Press Taylor & Francis Group, 2006.

[10] SUEMATSU Y, TSUNETA S, ICHIMOTO K, *et al*.. The solar optical telescope of solar-B: the optical telescope assembly [J]. *Solar Physics*, 2008, 249: 197-220.

[11] 辛雪军,陈长征,张星祥,等. 平行光管主反射镜组件的非线性有限元分析 [J]. 中国光学与应用光学, 2010, 3(2): 171-174.
XIN X J, CHEN CH ZH, ZHANG X X, *et al*.. Nonlinear analysis of primary mirror subassembly for collimator based on finite element method [J]. *Chinese J. Opt. Appl. Opt.*, 2010, 3(2): 171-174. (in Chinese)

[12] 刘伟. 小型 Offner 凸光栅光谱成像系统的结构设计及分析 [J]. 中国光学与应用光学, 2010, 3(2): 159-162.
LIU W. Design and analysis of structure of compact offner spectral imaging system [J]. *Chinese J. Optics Appl. Opt.*, 2010, 3(2): 159-162. (in Chinese)

Author's biographies: LIANG Biao (1985—), male, from Sichuan province, postgraduate, is specialized in optomechanical design and optimization analysis. E-mail: vbhj602@163.com

LIU Wei (1967—), male, from Jilin province, senior engineer, supervisor of master students, is specialized in fine mechanics design. E-mail: 2400liuwei@163.com

《中国光学》征稿启事

《中国光学》为双月刊,A4 开本; 刊号: ISSN 2095-1531/CN 22-1400/O4; 国内外公开发行,邮发代号: 国内 12-140,国外 BM6782。

★ 中国科技核心期刊
★ 中国光学学会光电技术专业委员会会刊
★ 中国学术期刊(光盘版)源期刊

报道内容:基础光学、发光理论与发光技术、光谱学与光谱技术、激光与激光技术、集成光学与器件、纤维光学与器件、光通信、薄膜光学与技术、光电子技术与器件、信息光学、新型光学材料、光学工艺、现代光学仪器与光学测试、光学在其他领域的应用等。

发稿类型: 学术价值显著、实验数据完整的原创性论文; 研究前景广阔,具有实用、推广价值的技术报告; 有创新意识,能够反映当前先进水平的阶段性研究简报; 对当前学科领域的研究热点和前沿问题的专题报告; 以及综合评述国内外光学技术研究现状、发展动态和未来发展趋势的综述性论文。

本刊已和国际知名组织达成合作办刊意向,因此,2012 年本刊只发表英文撰写的学术论文,欢迎投稿、荐稿。

主管单位: 中国科学院
主办单位: 中国科学院长春光学精密机械与物理研究所
编辑出版 《中国光学》编辑部
投稿网址: http://chineseoptics.net.cn
邮件地址: chineseoptics@ciomp.ac.cn; zggxcn@126.com
联系电话: 0431-86176852; 0431-84627061 传 真: 0431-84627061
编辑部地址: 长春市东南湖大路 3888 号(130033)